

OVERVIEW OF SASE EXPERIMENTS

P. Castro, DESY, Notkestrasse 85, 22603 Hamburg, Germany

Abstract

The radiation characteristics of Free Electron Lasers (FEL) based on the Self-Amplified Spontaneous Emission (SASE) principle are very high brilliance and full transverse coherence. These properties, together with the possibility to tune it to low wavelengths, make of SASE FELs a unique synchrotron radiation source type. Linac driven SASE FELs require high peak current electron pulses with very small transverse emittance. Photocathode RF guns and bunch compressors are indispensable linac components in order to achieve the high beam quality required. A very precise long magnetic undulator structure is also mandatory to provide the interaction between the photon field and the electron bunch. After a short introduction of the SASE principle and beam requirements, recent results of SASE experiments world wide will be given, focusing on the TESLA Test Facility results around 100 nm.

1 INTRODUCTION

The photon wavelength λ_{ph} of the first harmonic of Free Electron Laser (FEL) radiation [1] is related to the period length λ_u of a planar undulator by

$$\lambda_{\text{ph}} = \frac{\lambda_u}{2\gamma^2} \left(1 + \frac{K^2}{2} \right) \quad (1)$$

where $\gamma = E/m_e c^2$ is the relativistic factor of the electrons, $K = eB_u \lambda_u / 2\pi m_e c$ the 'undulator parameter' and B_u the peak magnetic field in the undulator. Eq. (1) exhibits two main advantages of the FEL: the free tunability of the wavelength by changing the electron energy and the possibility to achieve very short photon wavelengths.

For most FELs presently in operation [2], the electron beam quality and the undulator length result in a gain of only a few percent per passage, so that an optical cavity resonator and a synchronized multi-bunch electron beam have to be used. At very short wavelengths, normal-incidence mirrors of high reflectivity are unavailable.

The principle of SASE FEL [3, 4] is presently the most promising concept to extend the working principle of FELs to the VUV and X-ray wavelength regime. In a SASE FEL lasing occurs in a single pass of a relativistic, dense electron bunch through a long undulator magnet structure. In this 'high-gain' FEL an electron beam of extremely high quality in terms of emittance, peak current and energy spread, and a high precision undulator of sufficient length are essential. Provided that spontaneous radiation from the first part of the undulator overlaps the electron beam, the electromagnetic radiation interacts with the electron bunch leading to a density modulation (microbunch-

ing), which enhances the power and coherence of the radiation. In this "high gain mode" [5, 6, 7], the radiation power $P(z)$ grows exponentially with the distance z along the undulator

$$P(z) = P_o \cdot A \cdot \exp\left(\frac{2z}{L_g}\right) \quad (2)$$

where L_g is the field gain length, P_o the effective input power (see below), and $A = 1/9$ in one-dimensional FEL theory with an ideal electron beam. For very short wavelengths, there is no laser tunable over a wide range to provide the input power P_o . Instead, the spontaneous undulator radiation from the first part of the undulator is used as an input signal to the downstream part.

2 SASE PROOF-OF-PRINCIPLE EXPERIMENTS

X-ray lasers are expected to open up new and exciting areas of basic and applied research in biology, chemistry and physics. FELs based on this SASE principle are presently considered the most attractive candidates for delivering extremely brilliant, coherent light with wavelength in the Ångström regime [8, 9, 10, 11]. Compared to state-of-the-art synchrotron radiation sources, one expects full transverse coherence, larger average brilliance and, in particular, up to eight or more orders of magnitude larger peak brilliance at pulse lengths of about 200 fs FWHM. Within the last two years, three important proof-of-principle experiments have successfully demonstrated large SASE gain at shorter and shorter wavelengths: 12 μm wavelength was achieved 1998 at Los Alamos (here referred to as UCLA/LANL) [12], 530 nm wavelength was achieved 1999 at Argonne (LEUTL) [13], and 109 nm wavelength was achieved 2000 at DESY (TTF FEL) [14]. The main parameters for FEL operation are compiled in Table 1.

The basic accelerator components for all three SASE experiments are a low emittance photocathode rf electron gun, a linear accelerator based on high-gradient rf cavities and a long permanent magnet undulator. This paper focuses on the description of the experimental setup of the FEL at the TESLA Test Facility (TTF FEL) [15] at the Deutsches Elektronen-Synchrotron (DESY). The TESLA (TeV Energy Superconducting Linear Accelerator) collaboration consists of 39 institutes from 9 countries and aims at the construction of a 500 GeV (center-of-mass) e+e-linear collider with an integrated X-ray laser facility [10]. The layout of TTF Linac is shown in Fig. 1. Major hardware contributions to TTF have come from Germany, France, Italy and the USA.

Parameter	Units	UCLA/LANL[12]	LEUTL[13]	TTF FEL[14]
beam energy at undulator	MeV	18	217	233±5
rms energy spread	MeV	0.045	0.2	0.3±0.2
rms transverse beam size	μm	115-145	130	100±30
normalized emittance in the undulator	π mrad mm	?	5	6±3
electron bunch charge	nC	2	0.7	1
peak electron current	A	170	150	400±200
bunch spacing	ns	9.23	0.35	1000
repetition rate	Hz	1	10	1
λ_u (undulator period)	mm	20.5	33	27.3
undulator peak field	T	0.54	1.006	0.46
effective undulator length	m	2.0	12	13.5
λ_{ph} (radiation wavelength)	nm	12000	530	80 - 180
FEL gain		$3 \cdot 10^5$	$> 10^2$	$3 \cdot 10^3$
FEL radiation pulse length FWHM	ps	6	5	0.3 - 1

Table 1: Typical parameters of recent SASE FEL experiments.

TTF FEL is operating between 80 and 180 nm and is to date the FEL with the shortest wavelength. In a second phase, the goal is to build a soft X-ray user facility [16, 17].

3 TTF FEL EXPERIMENTAL SETUP

The injector for the TTF FEL is based on a laser-driven $1 \frac{1}{2}$ -cell rf gun electron source operating at 1.3 GHz [18]. The Cs₂Te cathode [19] is illuminated by a train of UV laser pulses generated in a mode-locked solid-state laser system [20] synchronized with the rf. An energy of up to 50 μJ with a pulse-to-pulse variation of 2% (rms) is achieved. The UV pulse length measured with a streak camera is $\sigma_t = 7.1 \pm 0.6$ ps. The gun section is followed by a 9-cell superconducting cavity, boosting the energy to 16 MeV.

The superconducting accelerator structure has been described elsewhere [21]. A bunch compressor is inserted between the two accelerating modules, in order to increase the peak current of the bunch up to $\hat{I} = 500$ A, corresponding to 0.25 mm bunch length (rms) for a 1 nC bunch with Gaussian density profile. Experimentally, it is routinely verified that a large fraction of the bunch charge is compressed to a length below 0.4 mm (rms) [22]. There are indications that the core is compressed even further. We estimate the peak current for the FEL experiment at (400 ± 200) A.

The undulator is a fixed 12 mm gap permanent magnet device using a combined function magnet design [23] with a period length of $\lambda_u = 27.3$ mm and a peak field of $B_u = 0.46$ T, resulting in an undulator parameter of $K = 1.17$. The beam pipe diameter in the undulator (9.5 mm) [24] is much larger than the beam diameter (300 μm). Integrated quadrupole structures produce a gradient of 10.4 T/m superimposed on the periodic undulator field in order to focus the electron beam along the undulator. The undulator system is subdivided into three segments, each 4.5 m long and containing 10 quadrupole sections to build up 5 full focusing-defocusing (F0D0) cells. The F0D0 lattice periodicity runs smoothly from segment to segment. There is

a spacing of 0.3 m between adjacent segments for diagnostics. The total length of the system is 14.1 m.

For optimum overlap between the electron and the radiated photon beams, high precision on the magnetic fields and mechanical alignment are required. The beam orbit straightness in the undulator is determined by the alignment precision of the superimposed permanent-magnet quadrupole fields which is better than 50 μm in both vertical and horizontal direction [25].

Different techniques have been used to measure the emittance of the electron beam [26] and yield values for the normalized emittance of $(4 \pm 1) \pi$ mrad mm for a bunch charge of 1 nC at the exit of the injector. The emittance in the undulator, as determined from quadrupole scans and from a system of wire scanners, was typically between 6 and 10 π mrad mm (in both horizontal and vertical phase space). It should be noted that the measurement techniques applied determine the emittance integrated over the entire bunch length. The slice emittance (i.e., the emittance of bunch slices much shorter than the bunch length) is, however, the relevant parameter for FEL physics. It is likely that, due to spurious dispersion and wakefields, the bunch axis is tilted about a transverse axis such that the projected emittance is larger than the emittance of any slice. Based on these considerations we estimate the normalized slice emittance in the undulator at $(6 \pm 3) \pi$ mrad mm.

For radiation intensity measurements we used a PtSi photodiode integrating over all wavelengths. The detector unit was placed 12 m downstream the undulator exit. A 0.5 mm iris was placed in front of the photodiode in order to avoid saturation effects. The photodiode can be removed to allow the photon beam till the spectrometer, which consists of a grid that can be rotated to select the range of wavelengths and a CCD camera.

In summary, it should be emphasized that full knowledge and control of the transverse and longitudinal phase space distribution of the electron beam is essential for SASE FEL

TTF FEL 1

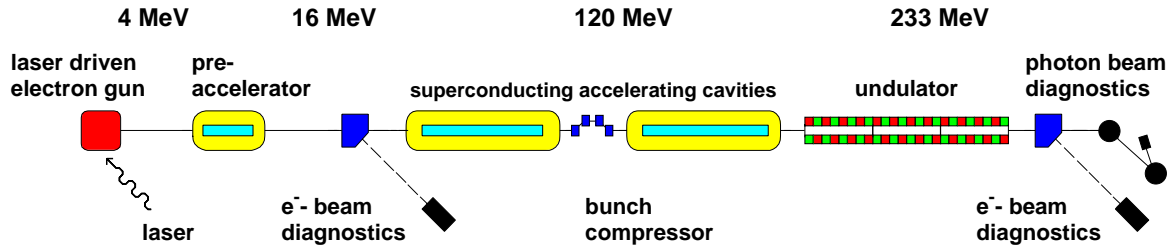


Figure 1: Schematic layout of phase 1 of the SASE FEL at the TESLA Test Facility at DESY, Hamburg. The linac contains two 12.2 m long cryogenic modules each equipped with eight 9-cell superconducting accelerating cavities [21]. The total length is 100 m.

operation. Parameters like peak current (i.e., bunch lengths in the 100 μm range) and slice emittance (for slices in the micrometer range) determine the SASE power exponentially. Thus, already modest uncertainties in the knowledge of these parameters can change the undulator length that is required to achieve FEL saturation by a factor of two or so. In particular in view of X-ray FELs, these requirements put new challenges to electron beam diagnostics.

4 FEL MEASUREMENTS

A strong evidence for the FEL process is a large increase in the on-axis radiation intensity if the electron beam is injected such that it overlaps with the radiation during the entire passage through the undulator. The observed intensity inside a window of $\pm 200 \mu\text{m}$ around the optimum beam position was enhanced by a factor of more than 100 compared to the intensity of spontaneous radiation observed outside this window.

SASE gain is expected to depend on the bunch charge in an extremely nonlinear way. Fig. 2 shows the measured intensity on axis as a function of bunch charge Q , while the beam orbit is kept constant for optimum gain. The solid line indicates the intensity of the spontaneous undulator radiation multiplied by a factor of 100. The strongly nonlinear increase of the intensity as a function of bunch charge is a definite proof of FEL action. The gain does not further increase if the bunch charge exceeds some 0.6 nC. This needs further study, but it is known that the beam emittance becomes larger for increasing Q thus reducing the FEL gain.

A typical wavelength spectrum of the radiation at TTF FEL (taken on axis at maximum FEL gain) is presented in Fig. 3. The central wavelength of 108.5 nm is consistent with the measured beam energy of (233 ± 5) MeV and the known undulator parameter $K = 1.17$, see eq. (1). The intensity gain determined with the CCD camera of the spectrometer is in agreement with the photodiode result.

A characteristic feature of SASE FELs is the concentration of radiation power into a cone much narrower than that of wavelength integrated undulator radiation, whose opening angle is in the order of $1/\gamma$. Measurements done by moving the 0.5 mm iris horizontally together with the

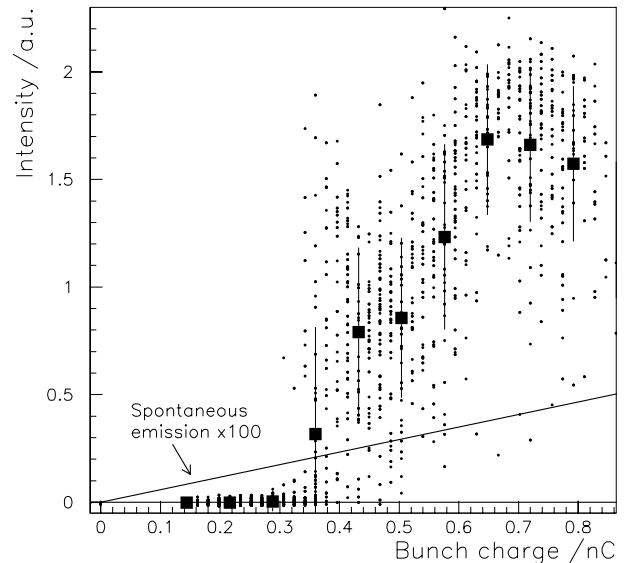


Figure 2: SASE intensity versus bunch charge. The straight line is the spontaneous intensity multiplied by a factor of 100. To guide the eye, mean values of the radiation intensity are shown for some bunch charges (dots). The vertical error bars indicate the standard deviation of intensity fluctuations, which are due to the statistical character of the SASE process, see eq. (3).

photodiode confirm this expectation, see Fig. 4. To be visible on this scale, the spontaneous intensity is amplified by a factor of 30. The energy flux is 2 nJ/mm^2 at the location of the detector and the on-axis flux per unit solid angle is about 0.3 J/sr (assuming a source position at the end of the undulator). This value was used as reference point for the numerical simulation of the SASE FEL with the code FAST [27]. Calculations have been performed for a Gaussian energy spread of 0.1%. The longitudinal profile of the bunch current was assumed to be Gaussian with an rms length of 0.25 mm. The transverse distribution of the beam current density was also taken to be Gaussian. The normalized emittance ε_n was varied in the simulations between 2 and $10 \pi \text{ mrad mm}$. Our calculations show that in this range of parameters the value of the effective power of shot

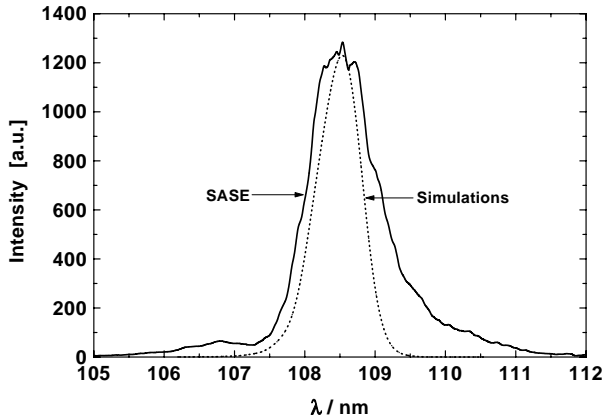


Figure 3: Wavelength spectrum of the central radiation cone (collimation angle ± 0.2 mrad), taken at maximum FEL gain. The dotted line is the result of numerical simulation. The bunch charge is 1 nC.

noise P_o and coupling factor $A \simeq 0.1$ (see eq. 2) are nearly constant. A level of energy flux of 0.3 J/sr is obtained at five field gain lengths L_g . With these parameters the FEL gain can be estimated at $G \approx 3 \times 10^3$ with a factor of 3 uncertainty (i.e., $10^3 < G < 10^4$) which is mainly due to the imprecise knowledge of the longitudinal beam profile. If we assume that the entire undulator contributes to the FEL amplification process, we estimate the normalized emittance ε_n at 8π mrad mm in reasonable agreement with the measurements. This value of the emittance was used for more detailed calculations of the FEL characteristics. Theoretical spectral and angular distributions as calculated by this numerical simulation are included in Figs. 3 and 4. In both cases the experimental curves are wider than the simulation results. A possible source of the widening is energy and orbit jitter of the electron beam, since the experimental curves are results of averaging over many bunches. This is confirmed by more recent measurements taken at improved energy stability, where the agreement with theory is much better. Large SASE gain was achieved in a stable and reproducible way for several weeks.

Similarly, a SASE gain as high as $G = 3 \cdot 10^5$ was demonstrated 1998 at Los Alamos at $12 \mu\text{m}$ wavelength [12], and the LEUTL experiment achieved a gain above 10^2 at 530 nm wavelength [13].

It is essential to realize that the fluctuations seen in Fig. 2 are not primarily due to unstable operation of the accelerator but are inherent to the SASE process. Shot noise in the electron beam causes fluctuations of the beam density, which are random in time and space [28]. As a result, the radiation produced by such a beam has random amplitudes and phases in time and space and can be described in terms of statistical optics. In the linear regime of a SASE FEL, the radiation pulse energy measured in a narrow central cone (with an opening angle of $\pm 20 \mu\text{rad}$ in TTF FEL) at maximum gain is expected to fluctuate according to a gamma distribution $p(E)$ [29],

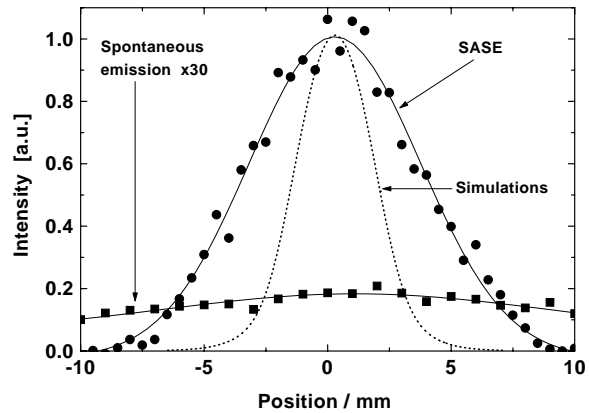


Figure 4: Horizontal intensity profile of SASE FEL and spontaneous undulator radiation ($\times 30$), measured with a photodiode behind a 0.5 mm aperture in a distance of 12 m from the end of the undulator. The dotted line is the result of numerical simulation.

$$p(E) = \frac{M^M}{\Gamma(M)} \left(\frac{E}{\langle E \rangle} \right)^{M-1} \frac{1}{\langle E \rangle} \exp \left(-M \frac{E}{\langle E \rangle} \right) \quad (3)$$

where $\langle E \rangle$ is the mean energy, $\Gamma(M)$ is the gamma function with argument M , and $M^{-1} = \langle (E - \langle E \rangle)^2 \rangle / \langle E \rangle^2$ is the normalized variance of E . The parameter M corresponds to the number of optical modes. Note that the same kind of statistics applies for completely chaotic polarized light, in particular for spontaneous undulator radiation.

For these statistical measurements the signals from 3000 TTF FEL radiation pulses have been recorded, with the small iris (0.5 mm diameter) in front of the photo diode to guarantee that transversely coherent radiation pulses are selected. Thus, the parameter M corresponds to the number of longitudinal modes. As one can see from Fig. 5, the distribution of the energy in the radiation pulses is quite close to the gamma distribution. The relative rms fluctuations are about 26% corresponding to $M = 14.4$.

One should take into account that these fluctuations arise not only from the shot noise in the electron beam, but the pulse-to-pulse variations of the beam parameters can also contribute to the fluctuations. Thus, the value $M \approx 14$ can be considered as a lower limit for the number of longitudinal modes in the radiation pulse. Using the width of radiation spectrum we calculate the coherence time [29] and find that the part of the electron bunch contributing to the SASE process is at least $100 \mu\text{m}$ long. From the quality of the agreement with the gamma distribution we can also conclude that the statistical properties of the radiation are described with Gaussian statistics. In particular, this means that there are no FEL saturation effects.

5 SUMMARY

SASE has become an unquestionable reality in the IR, visible and VUV wavelength regime, and reliable operation

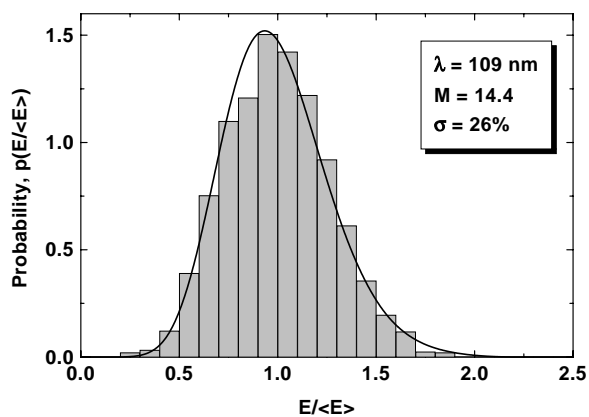


Figure 5: Probability distribution of SASE intensity. The rms fluctuation yields a number of longitudinal modes $M = 14$. The solid curve is the gamma distribution for $M = 14.4$. The bunch charge is 1 nC.

was demonstrated at DESY over several weeks. To date, all observations are in agreement with the present SASE FEL models, so optimism is justified that even shorter wavelengths will be reached in close future. It is essential that these experiments have been performed at different laboratories and with quite different setups. This indicates that the theory to understand SASE FEL and the technology to construct such facility have attained a rather mature level.

It should be clear, on the other hand, that there is still a way to go from present test facilities to X-ray user facilities. First, the SASE gain demonstrated so far is still some orders of magnitude below FEL saturation. Second, larger factors of bunch length compression are needed at shorter wavelengths without affecting the transverse beam emittance. Moreover, further development on electron beam diagnostics and eventually new techniques are required for better beam quality control. Finally, stable operation with long pulse trains containing several thousand pulses and flexible timing pattern, as requested by users, will remain a challenge for accelerator physicists for a while.

6 REFERENCES

[1] J.M.J. Madey, *J. Appl. Phys.* **42**, 1906 (1971).
 [2] W.B. Colson, *Nucl. Instr. and Meth.* **A429**, 37-40 (1999).
 [3] R. Bonifacio, C. Pellegrini, L.M. Narducci, *Opt. Commun.* **50**, 373 (1984)
 [4] A.M. Kondratenko, E.L. Saldin, *Part. Accelerators* **10**, 207 (1980)
 [5] K.J. Kim, *Phys. Rev. Lett.* **57**, 1871 (1986)
 [6] S. Krinsky, L.H. Yu, *Phys. Rev.* **A35**, 3406 (1987)
 [7] E.L. Saldin, E.A. Schneidmiller, M.V. Yurkov, "The Physics of Free Electron Lasers", Springer (1999) and references therein
 [8] H. Winick, et al., *Proc. PAC Washington and SLAC-PUB-6185*, (1993)
 [9] R. Brinkmann, et al., *Nucl. Instr. and Meth.* **A 393**, 86-92 (1997)

[10] R. Brinkmann, G. Materlik, J. Rossbach, A. Wagner (eds.), DESY 1997-048 and ECFA 1997-182 (1997)
 [11] H.-D. Nuhn, J. Rossbach, *Synchrotron Radiation News* **13**, No. 1, 18 - 32 (2000)
 [12] M. Hogan et al., *Phys. Rev. Lett.* **81**, 4867 (1998)
 [13] S. Milton et al., "Observation of Self-Amplified Spontaneous Emission and Exponential Growth at 530 nm", submitted to *Phys. Rev. Lett.* (2000)
 [14] J. Andruskow et al., "First Observation of Self-Amplified Spontaneous Emission in a Free-Electron-Laser at 109 nm Wavelength", submitted to *Phys. Rev. Lett.* (2000)
 [15] W. Brefeld et al., *Nucl. Instr. and Meth.* **A393**, 119-124 (1997)
 [16] T. Åberg et al., "A VUV FEL at the TESLA Test Facility at DESY", Conceptual Design Report, DESY Print TESLA-FEL 95-03 (1995)
 [17] J. Rossbach, *Nucl. Instr. and Meth.* **A 375**, 269 (1996)
 [18] J.-P. Carneiro, et al., *Proc. 1999 Part. Acc. Conf.*, New York, 2027-2029 (1999)
 [19] P. Michelato, et al., *Nucl. Instr. and Meth.* **A445**, 422 (2000)
 [20] I. Will, S. Schreiber, A. Liero, W. Sandner, *Nucl. Instr. and Meth.* **A445**, 427 (2000)
 [21] H. Weise, *Proc. 1998 Linac Conf. Chicago*, 674-678 (1998)
 [22] M. Geitz, G. Schmidt, P. Schmüser, G.V. Walter, *Nucl. Instr. and Meth.* **A445**, 343 (2000)
 [23] Y.M. Nikitina, J. Pflüger, *Nucl. Instr. and Meth.* **A375**, 325 (1996)
 [24] U. Hahn, et al., *Nucl. Instr. and Meth.* **A445**, 442 (2000)
 [25] J. Pflüger, *Nucl. Instr. and Meth.* **A445**, 366 (2000)
 [26] H. Edwards, et al., *Proc. 1999 FEL Conf, Hamburg*
 [27] E.L. Saldin, E.A. Schneidmiller, M.V. Yurkov, *Nucl. Instr. and Meth.* **A 429**, 233 (1999)
 [28] R. Bonifacio, et al., *Phys. Rev. Lett.* **73**, 70 (1994)
 [29] E.L. Saldin, E.A. Schneidmiller, M.V. Yurkov, *Opt. Commun.* **148** 383 (1998)